

## Remediation of Pool Dominated Trichloroethene Source Zones in Heterogeneous Porous Media by Cosmetic Surfactant Flooding

Gokce Akyol<sup>1\*</sup>, Cafer Ozkul<sup>1</sup>, Seda Karayunlu Bozbaş<sup>2</sup>, Nihat Hakan Akyol<sup>3</sup>

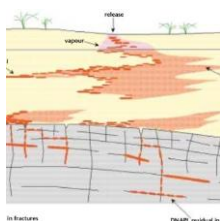
<sup>1</sup>Dumlupınar University, Department of Geological Engineering, Kutahya TURKEY

<sup>2</sup>Kocaeli University, Department of Chemistry, 41380, Kocaeli TURKEY

<sup>3</sup>Kocaeli University, Department of Geological Engineering, 41380, Kocaeli TURKEY

\*Corresponding author: gokce-81@hotmail.com

### GRAPHICAL ABSTRACT



### Abstract

A series of flow-cell experiments were performed to investigate the performance of cosmetic rhamnolipid surfactant flooding on the relationship between source zone mass removal and mass flux reduction for pool-dominated DNAPL TCE source zones in heterogeneous porous media. The results were also compared to those of water-flood control experiments to assess the surfactant enhanced flushing efficacy. The flooding experiments were performed for silica sand and natural calcareous soil representing two different degrees of physical heterogeneity. The result from the flow-cell experiments showed that higher than 97% of TCE mass was removed during rhamnolipid flooding for both porous media scenarios. Although, rhamnolipid flooding experiment results showed successful remediation performance, DNAPL TCE dissolution and rhamnolipid-enhanced dissolution in heterogeneous porous media system exhibited multi-step mass-flux reduction/mass-removal behavior due to the presence of less hydraulically-accessible pool-dominated TCE source zone. However, mass removal and mass-flux reduction relationships for rhamnolipid flushing cases exhibited more ideal removal behavior, indicating the more efficient remediation performance compared to water flooding alone. For all cases, the later stage of mass removal was controlled by the more poorly-accessible mass associated with pool-dominated source zones. The results of this

study revealed the impact of non-uniformity of the flow-field and effect of enhanced-solubilization agent on mass removal and mass-flux reduction behavior for DNAPL source zones in saturated porous media

**Keywords:** Cosmetic surfactant, Dissolution, DNAPL, Mass flux, Rhamnolipid, Trichloroethene

## 1. Introduction

Non-aqueous phase liquids (NAPL) are generally classified according to their liquid density compared to water, so NAPL that are less dense than water is classified as LNAPL and those denser than water as DNAPL. Most fuel derivatives and petroleum hydrocarbons are classified as LNAPL. Solvents and solvent stabilizers are predominantly represented as DNAPL (Booth et al., 2019). Dense non-aqueous phase liquids (DNAPL) are chemical or chemical mixtures that are poorly soluble in water. Due to these two properties, they can move downward and accumulate into soil and groundwater when a sufficient amount is released into the environment. Under such conditions, the movement of DNAPL will continue until they encounter a resistant or low permeability layer. In this process, their path may be complicated, as they will prefer the path with least resistance in subsurface soils (USEPA, 2020).

Due to the high toxicity and persistence of DNAPL in the environment, they can seriously contaminate subsurface areas and groundwater resources for many years to decades. Therefore, it is of critical importance to improve the remediation strategies for DNAPL source zones in order to maintain or restore the water quality of aquifer systems. Effectively removing DNAPL source regions from the subsurface (groundwater) is one of the most difficult processes facing remediation (Akyol, 2018).

There are many techniques for DNAPL remediation; Pump-and-treat (PT) technology is commonly used has been shown to have limited effectiveness for DNAPL mass removal, because of the high density, low solubility, and high interfacial tension of DNAPL with water (Akyol et al., 2013; Booth et al., 2019; USEPA, 2020). In situ enhanced-solubilization remediation techniques have focused on the use of flushing agents (for instance surfactants, cosolvents, and cyclodextrins) to reduce the interfacial tension between the DNAPL and water

and to increase the apparent solubility of organic pollutants (Difilippo et al., 2010; Akyol et al., 2013; Tick et al., 2015; Akyol, 2018; Akyol and Turkkan, 2018).

Therefore, surfactant-enhanced aquifer remediation (SEAR) and other enhanced-solubilization methods have been used to increase contaminant-mass removal for such systems. SEAR is based upon two primary removal mechanisms: (1) mobilization of trapped NAPL caused by interfacial tension reduction; and (2) micellar solubilization (Booth et al., 2019; Akyol et al., 2013; Akyol, 2018; Akyol and Turkkan, 2018).

Due to potential issues with mobilization of DNAPL, solubilization-based remediation methods have gained significantly more attention. Based on the micelle-based removal mechanism of surfactants to enhance solubilization of organics, significant solubilization will only occur when surfactant concentrations are higher than its critical micelle concentration (CMC) (Akyol et al., 2013; Ghosh et al., 2015; Zhong et al., 2016). Because of this reason, most of the studies focused on NAPL remediation, have been performed at relatively higher CMC surfactant concentrations. For instance, various types of surfactants used for enhanced-solubilization of chlorinated solvents (i.e., DNAPL) at higher CMC concentrations are observed in the literature (Harendra and Vipulanandan, 2011). The remediation of NAPL from porous media using surfactant concentrations above CMC have also been investigated under flowing system conditions (Boving and Brusseau, 2000; Zhong and Oostrom, 2012). There have been two major challenges encountered for this application: (1) introduction of large amounts of surfactant into the aquifer, which may cause secondary contamination or other impacts to the system; and (2) potential effect on distribution and migration of NAPL via mobilization. These phenomena have the potential to have significant negative impacts on the efficacy of the SEAR technology.

Some prior studies have shown that solubilization may also occur when surfactant concentrations are lower than the CMC (Kile and Chiou, 1989; Zhang and Miller, 1992). Specifically, it was shown that rhamnolipid biosurfactants exhibited strong alkane-solubilization activity at concentrations significantly lower than CMC, through an aggregate-formation mechanism (Zhong et al., 2016). In addition, synthetic surfactants, SDBS and TX-100, were observed to enhance the solubility of hexadecane at concentrations below their

CMC (Zhong et al., 2015). The prior studies also indicated that bioremediation was possible for the remediation of contaminants via biosurfactants.

Chemical flooding with bio-active agents can be used to remediate soil and groundwater contaminated with DNAPL. Biosurfactants reduce the interfacial tension between water and NAPL and increase the mobilization and the solubility of organic compounds. Thus, the pollutant can be remediated from the subsurface at an accelerated rate. For instance, rhamnolipid is a microorganism that produces a glycolipid biosurfactant that was used for the bioremediation of DNAPL source zones (Strbak, 2000; Mata-Sandoval et al., 2001).

The interest in biosurfactants, which are often called surface active biological agents due to their specific environmental properties, is increasing all over the world. There are five main categories of biological surfactants. These are glycolipids, phospholipids and fatty acids, lipopeptides and lipoproteins, polymeric bio-surfactants and particulate bio-surfactants (Xu et al., 2011; Randhawa and Rahman, 2014)

This is where the current global interest in Rhamnolipid production lies, due to its wide range of applications in various industries and its impressive "environmental" properties. The list of five major rhamnolipid applications meeting broad industrial requirements includes: Bioremediation and enhanced oil recovery (EOR), Pharmaceuticals and therapeutics, Cosmetics, Detergents and cleaners, Agriculture (Sajna and Gottumukkala, 2019).

Glycolipid biosurfactants 'rhamnolipids' are distinguished between the different types of bio-surfactants. Rhamnolipid is mainly a crystalline acid consisting of  $\beta$ -hydroxy fatty acid linked with the rhamnose sugar molecule via the carboxy end member (functional group). *Pseudomonasaeruginosais* is mainly formed with rhamnolipids and is graded as mono and dirhamnolipids. *P. chlororaphis*, *P. plantarii*, *P. putida*, and *P. fluorescens* have been identified for the production of rhamnolipids. Certain bacteria produce mono-rhamnolipids only, while others produce both. In the production method, the ratio of mono and dirhamnolipid may also be controlled (Sajna and Gottumukkala, 2019).

There has been a large body of research on rhamnolipids over three decades, revealing many novel applications, making them a promising alternative and a popular choice for remediation

efforts among all biosurfactant categories worldwide. Because of their wide range of applications in cosmetic industries and their impressive "environmental" properties, the current global interest in rhamnolipid manufacturing and their application value has increased over time. A list of five main rhamnolipid applications that meet the broad range of industrial requirements include: bioremediation and enhanced oil recovery (EOR) (Xue et al., 2020; Rathankumar et al., 2021) pharmaceuticals and therapeutics (Yi et al., 2019; Thakur et al., 2021) cosmetics (Ahmadi-Ashtiani et al., 2020) detergents and cleaners (Jadhav et al., 2019; Helmy et al., 2020) Agriculture (Chen et al., 2017; Dashtbozorg et al., 2019).

There is a current lack of studies in the literature regarding the use of rhamnolipid surfactant for the remediation of DNAPL. The use of rhamnolipid for soil leaching and enhanced biodegradation of LNAPL have been successfully applied associated remediation efforts. However, there have been no significant studies regarding the effect of rhamnolipid biosurfactant on the remediation of pool dominated DNAPL source zones. Prior studies have primarily investigated the solubilization potential of chlorinated solvents (i.e., DNAPL) using biosurfactants and synthetic surfactants such as SDS and Tween 80 (Difilippo et al., 2010; Akyol et al., 2013) Albino and Nambi (2019) showed that rhamnolipid biosurfactant was 4 times more effective at DNAPL removal, in terms of weight solubilization ratio (WSR), than Tween 80 for the solubility enhancement of TCE and PCE (i.e., two of the most encountered chlorinated solvents in contaminated sites). The objectives of a study present by Tang et. al. (2020) were to (1) evaluate the PCE degradation efficiency by the addition of rhamnolipid and Tween 80, and (2) investigate changes in microbial associations due to the addition of these two surfactants. This study showed that the type of surfactant added to the system was associated with changes in the microbial community and provided evidence for possible links between the degradation rates of PCE with two surfactants and changes in the microbial community structure. This has helped us to understand the current state of microbial ecology for the surfactant-enhanced bioremediation of PCE. As a result, synthetic surfactants have been predominantly used for the remediation of pool dominated DNAPL source zones and there has been lack of biological surfactants which was extensively used in cosmetic sector.

The objective of this study was to investigate the contaminant elution behavior and the impact of rhamnolipid cosmetic surfactant flooding on mass removal and mass-flux reduction relationships for non-uniform DNAPL TCE distributions entrapped within heterogeneous

porous media with within 2-D flow-cell systems. Two physically heterogeneous systems were utilized for determining the remediation efficacy due to the application of cosmetic rhamnolipid surfactant flooding techniques. Water flooding experiments were conducted as a control baseline conventional flushing technique (i.e, pump-and-treat technology) to compare and assess the performance of the novel SEAR technique.

## 2. Materials and Methods

A series of flow-cell experiments was conducted to test the impacts of porous media heterogeneity and non-uniform NAPL distribution on elution and mass-removal relationships under various rhamnolipid flooding scenarios. The rectangular tank was constructed of stainless steel and tempered glass, with dimensions of 40 cm (length) by 20 cm (width) by 3 cm (thick). This flow cell was equipped with multiple, evenly spaced injection/extraction ports on each end (inflow and outflow ends). In addition, three ports were evenly spaced at the top of the flow cell to allow injection of organic liquid (DNAPL). Water-tight seals were established using silicone sealant for the flow cell, ensuring that the tempered glass and flow cell body did not leak at any time during flushing. Two different silica-sand media median particle diameters,  $d_{50} = 0.359$  mm (40/50 mesh) and 0.172 mm (70/100 mesh), and natural calcareous soil were used in these experiments ( $d_{50}=0.12$  mm). The calcareous soil has a poorly sorted sandy loam texture with a mean grain diameter of 0.12 mm. This soil has an alkaline in nature with a pH of 8.4 and is characterized by the presence of abundant amounts of carbonate (96%) and intermediate amounts of organic carbon (1%) and minor amounts of quartz (Akyol and Yolcubal, 2013). The organic carbon content of silica sand materials is extremely low (O.C.%=0.05).

Trichloroethene (TCE), ACS grade (Aldrich Co.) was used as the model organic liquid (DNAPL), rhamnolipid was used as the cosmetic biosurfactant (Sigma-Aldrich Co.) for enhanced-solubilization flushing, and water alone was used as the conventional (pump-and-treat) flushing agent. Concentrations of rhamnolipid were selected as 2.5% and 5% wt. %) for the experiments. The organic liquid was dyed with Sudan IV (Aldrich Co.) at a concentration of 100 mg/L, which has been shown to have minimal impact on fluid properties and behavior (Schwille and Pankow, 1988; Kennedy and Lennox, 1997).

Two physical heterogeneous porous media configurations were constructed for the flow-cell experiments. The first flow-cell media configuration was comprised of a homogeneous pack

of the 40/50-mesh sand as the matrix, with a layer of the 70/100-mesh sand emplaced along the bottom boundary (Fig. 1). The second media configuration consisted of a matrix of the natural calcareous soil with two lenticular lenses of <200-mesh calcareous soil emplaced with the flow zone, and the <200-mesh calcareous soil was emplaced along the bottom boundary of the flow cell (Fig. 1). The <200-mesh calcareous soil prepared by sieving a natural calcareous soil and correspondingly used to construct the impermeable zones (low-permeability) for the second physical heterogeneous media configuration. As shown in Table 1, various locations of DNAPL TCE injections were applied and allowed to distribute within the flow cell medium for 48 hours. After 48 hours, the rhamnolipid surfactant or water was injected at a steady-state flow rate, equivalent to an average pore-water velocity of approximately 6.1 or 6.5 cm/h during reagent flooding to test the overall enhanced solubilization and remediation (removal) performance of DNAPL (TCE) source zones within the flow cell. This velocity range was selected to represent induced-gradient conditions associated with hydraulic-based remediation methods. NAPL saturation ( $S_n$ ) is defined as the volume of organic liquid divided by the pore volume of the entire system. Ten sets of experiments were conducted for the first and second flow-cell configurations using silica sand and natural calcareous soil. Experimental conditions and the type of DNAPL (TCE) injections are provided in Table 1. The initial distributions of DNAPL (TCE) generated for the two systems are shown in Figure 1.

The pool-dominated DNAPL (TCE) was injected into the 70/100-mesh sand or <200-mesh calcareous soil zone via the left and/or middle port (Fig. 1). Upon rhamnolipid flushing, effluent samples were collected (outflow side of flow cell) with 0.5 mL of glass syringe and an appropriate amount was transferred into a 5 mL flask (and diluted as necessary) for analysis. The aqueous samples were analyzed using ultraviolet-visible spectrophotometer (Varian Cary 150) at a wavelength of 230 nm (quantifiable detection limit of ~0.5 mg/L). Dilution of the rhamnolipid surfactant was not necessary to overcome interference for the analysis since the effect of rhamnolipid on TCE absorbance was negligible. TCE effluent samples were analyzed, and mass recoveries were calculated to determine the percent of TCE removed and for determining remediation efficacy. Although many studies only calculate the mass removal rate as a primary remediation efficacy metric, under such scenarios this may not provide enough detail to fully assess the performance of remediation efficacy. Therefore,

mass-flux-reduction/mass-removal analyses were performed to provide more comprehensive assessment of remediation efficacy.

Mass-flux-reduction/mass-removal behavior was simulated based on treating changes in mass-flux as a direct function of the change in contaminant mass (Dilippo et al., 2010; Akyol et al., 2013; Tick et al., 2015).

$$MFR = 1 - \frac{J_f}{J_i} = 1 - \frac{Q_f C_f}{Q_i C_i}$$

where  $J$  is mass-flux [M/t],  $M$  is source-zone mass [M] and the subscripts  $i$  and  $f$  represent initial and final, respectively.

### 3. Results and Discussion

#### 3.1. Contaminant elution behavior

The contaminant elution curves obtained from the flow-cell experiments are presented in Figures 2 and 3 for both silica sand and natural calcareous soil configurations. Ten set of experiments were conducted for silica sand and natural calcareous soil, respectively (Table 1).

For the first experiment 0.5 mL of TCE was injected as a pool within the 70/100-mesh sand followed by the flushing of a 5-wt.% rhamnolipid solution (Fig. 1). TCE effluent concentrations reached a maximum of 2456 mg/L and then decreased to 650 mg/L, reaching equilibrium (pseudo steady-state condition) for 4 hours. This phase was followed by a sharp decrease of TCE concentration over the duration of rhamnolipid flushing (Fig. 2). After a total of 11.5 hours of flushing, TCE concentrations dropped below 1 mg/L. For the second experiment 0.5 mL of TCE was injected into the left and middle ports as pools with equal mass within the medium and followed by the flushing of a 5-wt.% rhamnolipid solution. TCE reached a maximum concentration of 1906 mg/L and gradually decreased to 850 mg/L, followed by a constant pseudo steady-state effluent concentration for 3 hours (Fig 4). TCE dropped below 1 mg/L after 9 hours of flushing. The second experiment took less time (2.5 hours shorter) to reach TCE detection limits compared to the first experiment indicating that a higher dissolution rate (removal rate) for the TCE source zone occurred and may be related to more hydraulically accessible mass in this flow cell configuration. This phenomenon indicates



that a smaller amount of pool-dominated TCE source zone was removed for Experiment-1 compared to the more efficient (higher) removal observed for Experiment-2. The third flow cell experiment was the replication of Experiment-1 with the injection of 0.25 mL of TCE as the DNAPL pool. The TCE effluent concentrations reached a maximum of 1420 mg/L and decreased to 950 mg/L, followed by concentration stabilization (pseudo steady-state) for 3 hours. After 9 hours of flushing, TCE concentrations dropped below 1 mg/L (Fig 2). This experiment indicated the relatively lower amount of TCE injected into the system yielded improved remediation efficacy (faster removal rate) under the conditions of the experiment herein.

For the fourth experiment 0.25 mL of TCE (DNAPL) was injected within 70/100-mesh sand as a pool, followed by 2.5-wt.% solution of rhamnolipid surfactant flushing. Effluent concentrations of TCE reached a maximum of 788 mg/L followed by a gradual concentration decrease to 165 mg/L during flushing. After 11 hours of flushing, TCE concentrations dropped to 1 mg/L (Fig 2). This experiment (Exp-4) took almost 2 hours longer than the Experiment 3 with higher surfactant concentration (5%), indicating the reduced remediation (removal) efficacy impact associated with the lower surfactant concentration (i.e., decreased enhanced solubilization effect) for this remediation scenario. The fifth experiment (Experiment-5) was the replication of experiment 1 and 2 in terms of TCE source zone injection routine. Location and mass of TCE was kept same for experiment 1, experiment 2 and experiment 5, respectively. As mentioned previously, water was used as the flushing agent to represent conventional pump and treat remediation strategies. The control experiments under water flooding scenarios showed that effluent TCE concentrations reached a maximum value ~370 mg/L followed by an extensive stable (pseudo steady-state condition) concentration phase. It was observed that the initial TCE effluent concentrations were lower than its aqueous solubility limit (~1300 mg/L) due to the dilution effects resulting for the flow-cell experiments. The control experiments indicated that TCE effluent concentrations remained above 40 mg/L even after 80 PV of water flushing. This result clearly demonstrates the improved remediation efficacy of the rhamnolipid enhanced flooding technology compared to the conventional pump-and-treat scenarios. The water flushing control experiments also showed that an observed multi-step TCE elution behavior, similar to that observed for rhamnolipid flushing experiments. Similar elution behavior has also been observed for other enhanced-solubilization agents such as cyclodextrin (Akyol and Turkkan,

2018), Tween 80 (Difilippo et al., 2010) and SDS (Akyol, 2018) compared to water flushing scenarios for heterogeneous porous media systems.

The second series of flow cell experiments was conducted using a physically heterogeneous porous medium of calcareous soil. For the first experiment 0.5 mL of TCE was injected as a pool within the medium via the middle port followed by flushing of a 5-wt.% rhamnolipid solution. TCE effluent concentrations reached a maximum value of 2221 mg/L and decreased to 1000 mg/L whereby a stable concentration phase (pseudo steady state) and quasi-equilibrium state lasted for approximately 2 hours. After this temporal steady state phase, TCE elution concentrations gradually decreased during the rhamnolipid surfactant flushing and after 13 hours of total flushing time TCE concentrations dropped below 1 mg/L (Fig. 3). For the second experiment 0.5 mL of TCE was injected into left and middle ports to create DNAPL pools with equal mass and then followed by flushing the flow cell domain with a 5-wt.% rhamnolipid solution. Aqueous TCE effluent concentrations reached a maximum value of 1762 mg/L and slowly decreased to 1000 mg/L whereby a subsequent quasi-steady-state concentration elution period occurred for approximately 2 hours. After this elution phase, the effluent TCE concentrations dropped below 1 mg/L after 10.7 hours of total flushing time (Fig. 3). This second experiment took less time (~2.5 hours shorter) to reach TCE detection limits compared to the first experiment most likely due to the fact that the DNAPL mass was injected as a smaller pool than that of the previous (first experiment). The TCE pool distribution, under this scenario, may have yielded conditions more conducive to more hydraulically accessible mass and increased enhanced solubilization of TCE. In many cases a reduction of DNAPL pool size reduces the overall interfacial DNAPL area that would limit dissolution to a greater extent. The third experiment was a replication of experiment 2 but with an injection volume of 0.25 mL for the DNAPL TCE. The TCE effluent concentrations reached a maximum value of 1345 mg/L and decreased to 500 mg/L whereby a subsequent concentration stabilization (pseudo steady state) phase occurred for ~4 hours. After 9 hours for total surfactant flushing, TCE concentrations dropped below 1 mg/L (Fig. 3). For the fourth experiment TCE was injected into middle port as a DNAPL pool in the porous medium, and then followed by flushing of a 2.5-wt.% rhamnolipid solution. Effluent TCE concentrations reached a maximum value of 711 mg/L and decreased to 500 mg/L whereby a subsequent concentration stabilization (pseudo steady-state elution) period lasted for 2.5 hours (during flushing). After 11 hours of total flushing time TCE concentrations dropped below 1

mg/L at which point the experiment was concluded. This experiment indicated that the remediation performance of TCE was less effective compared to Experiment 3 due to the decreased enhanced-solubilization effect associated with the lower rhamnolipid 2.5-wt.% concentration.

The fifth experiment was the replication of experiment 1 and 2, in terms of location and distribution of TCE source zone condition. Instead of surfactant flooding, water was used as the flushing agent as a control flushing scenario representing conventional pump-and-treat operations. The control experiments under water flooding showed that effluent TCE concentration reached a maximum value of 180 mg/L, followed by an extensive stable concentration (pseudo steady-state) phase for a long period of time (Fig. 3). It is observed that initial effluent TCE concentrations were lower than its aqueous solubility limit (~1300 mg/L) due to the dilution effects associated with the flow cell experiments. The control experiments indicated that TCE effluent concentrations remained above 20 mg/L even after 100 PV of water flushing. This result clearly demonstrates the improved remediation efficacy of the rhamnolipid enhanced flooding technology compared to the conventional pump-and-treat scenarios, similar to that observed for the silica sand experiments.

All flow cell experiments for both physical configurations (silica sands and calcareous soils) showed that the TCE elution curves from dissolution and enhanced-solubilization of DNAPL were characterized by an extended multi-step behavior elution profile (Fig. 2 and Fig. 3). The presence of hydraulically-accessible (matrix) and poorly-hydraulically-accessible DNAPL pool zones is likely the primary control (phenomenon) causing this multi-step elution behavior. The TCE elution curves observed for the rhamnolipid flushing dissolution experiments exhibited relatively extensive periods wherein the TCE concentrations increased to a maximum value and then decreased gradually before reaching a long steady-state (quasi-equilibrium) elution concentration phase. This phase was followed by rapid decrease in TCE concentration until detection limits were reached around 0.5-1 mg/L. The extent of the steady-state TCE elution stages after first concentration dropped varied as a function of porous media, initial TCE saturation, location of TCE injection, and the type of flushing agent (i.e., rhamnolipid vs. water). The TCE mass associated with the less hydraulically accessible, higher-saturation region above the 70-100 silica sand or <200 mesh calcareous soil was the last portion to be removed and explains the steady-state TCE elution concentration behavior for the series of flushing experiments. This multi-step elution behavior is also consistent with

that observed in previous dissolution studies using ideal and non-ideal porous media (Mahal et al., 2009; Russo et al., 2010; Akyol et al., 2013; Akyol and Turkkan, 2018; Akyol, 2018). It is hypothesized that the pore-scale configuration of the organic liquid, DNAPL saturation, and the flow relationships are complex for both the silica sand and natural porous media experiments, resulting in the observed non-ideal dissolution and elution behavior. As a result, the performance of the enhanced-surfactant flushing technology depends on the site characteristics which are critical to determine the efficacy of these remediation strategies for NAPL-contaminated sites.

### 3.2. Mass-flux-reduction/mass removal behavior

The flow-cell experiments showed that the mass-flux reduction/mass removal (MFR/MR) relationships for various physically heterogeneous media configurations, the amount and the distribution of organic liquid, and the concentration of enhanced-solubilization reagent exhibited “multi-step” behavior. Multi-step behavior consists of two distinct MFR/MF stages. For the first stage, significant reductions in mass-flux occurred until minor fractions (15-20%) of mass were removed (Fig. 4 and Fig. 5). The mass-flux reduction/mass removal relationship was generally linear until a point at which approximately 70-75 % of mass was removed, as observed for most of the experiments using both the silica sand and natural calcareous soil porous media. The organic liquid (DNAPL-TCE) mass representing the more hydraulically-accessible zones (portions) was removed in this period for both the single and double DNAPL TCE injection experimental scenarios. This multi-step behavior is also similar with other enhanced solubilization agents with Tween 80 and Sodium dodecyl sulfate (SDS) surfactants with similar conditions (Akyol et al., 2013; Akyol, 2018; Akyol and Turkkan, 2018).

This multi-step behavior was also observed for the contaminant elution curves, whereby concentrations increased to a maximum and then decreased gradually until reaching a pseudo steady-state concentration condition for the majority of the surfactant flooding event. The mass-flux reduction/mass removal behavior observed for the silica sand flow cell configuration during water flushing (i.e., absence of rhamnolipid) exhibited more non-ideal removal behavior, indicating that dissolution processes are limited to a greater extent due to the organic liquid distribution and the absence of enhanced solubilization processes (Fig. 4). The MFR/MR removal behavior observed for the natural calcareous soil flow cell configuration during rhamnolipid flooding was significantly different that resulting from water flushing, exhibiting more non-ideal removal relationships compared that generated for

the silica sand configuration (Fig. 4 and Fig. 5). However, the MFR/MR relationships for rhamnolipid flushing cases generally exhibited more ideal removal behavior compared to water flooding, further indicating the more efficient remediation efficiency associated with the surfactant flushing. The final stage of MFR/MR reflects the removal of poorly-accessible organic liquid (DNAPL) mass from the entrapped pool distributed at the top of impermeable zone within the flow cell. The multi-step MFR/MR behavior was also observed for water flooding control experiments which has also been observed in prior flow-cell experiments and field-scale remediation demonstrations (Mahal et al., 2009; Russo et al., 2010; Akyol et al., 2013; Brusseau et al., 2013; Akyol and Turkkan, 2018; Akyol, 2018). Overall, these experiments show that the type of porous media, the various organic liquid distribution, the DNAPL saturation, and rhamnolipid surfactant concentration exhibit important impacts on DNAPL dissolution that may cause such non-ideal mass-flux reduction/mass removal behavior as observed and described in this section. This non-ideal (MFR/MR) removal behavior is hypothesized to occur from constraints related to hydraulic accessibility of the organic liquid to flowing water that will be implicitly controlled by pore-scale configuration of the flow-field and the impact of the enhanced-solubilization reagents on the source-zone dissolution processes. Such impacts of flow-field configuration on organic liquid dissolution have also been reported by prior dissolution studies that have used water and surfactants as the flushing reagents (Mahal et al., 2009; Russo et al., 2010; Akyol et al., 2013; Brusseau et al., 2013; Akyol and Turkkan, 2018; Akyol, 2018).

#### 4. Summary

Chlorinated solvents represent one of the main types of DNAPL frequently present contaminated sites throughout the world. These DNAPL sources can lead to severe soil and groundwater contamination. A series of flow-cell experiments was conducted to investigate the impact of non-uniform organic-liquid (NAPL) distribution, flow-field nonuniformity due to porous media physical heterogeneity, and enhanced-solubilization flushing agent (surfactant) concentration on the contaminant elution behavior and relationships between source zone mass removal and mass-flux reduction. Water flushing was conducted as the control experiments for dissolution of NAPL source zone removal, representing that of conventional pump-and-treat scenarios. A cosmetic rhamnolipid surfactant was successfully used for the remediation of DNAPL-TCE source zones established within the flow cell experiments. The results of the flow-cell experiments demonstrated that greater than 97% of

TCE mass was removed via rhamnolipid surfactant flooding. Experimental results also showed that the distribution and the emplacement of organic liquid (DNAPL-TCE), the flow-field nonuniformity, the particular concentration of rhamnolipid surfactant, and the porous media type (physical heterogeneity differences) significantly influenced on mass-flux reduction/mass removal behavior during flushing. The results of the study also showed that physical heterogeneous porous media systems using both silica sand and natural calcareous soil exhibited multi-step mass-flux reduction/mass removal relationships. However, mass removal and mass-flux reduction relationships for the rhamnolipid surfactant flushing cases exhibited more ideal contaminant mass removal behavior compared to water flooding, clearly demonstrating the more efficient and preferred remediation condition associated with the surfactant flushing scenario. Finally, the results of this study also reveal that during the earlier stages of flushing, a more efficient contaminant mass removal condition occurs likely due to a more hydraulically-accessible initial portion of DNAPL whereas during the later stages of flushing mass removal was predominantly controlled by the more poorly-accessible mass associated with higher-saturation DNAPL zones. Thus, it is important to note that such variations of NAPL hydraulic accessibility during flushing will most likely complicate the estimation and prediction of these remediation efforts. Studies such as the one herein aims to improve our understanding of contaminant dissolution and mass-flux behavior for the presence of organic liquid (NAPL) source zones in the subsurface in order to yield more robust site characterization and more efficient site remediation.

#### **Acknowledgements**

This study was funded by Kocaeli University Research Fund Project No: FHD-2020-2169.

#### **Data Availability**

We will provide data sets upon request from corresponding author.

#### **Disclosure statement**

No potential competing interest was reported by the authors.

#### **References**

U.S. EPA Office of Superfund Remediation and Technology Innovation

- Ahmadi-Ashtiani H.R., Baldisserotto A., Cesa E., Manfredini S., Zadeh H.S., Gorab M.G., Khanahmadi M., Zakizadeh S., Buso P., Vertuani S., Microbial Biosurfactants as Key Multifunctional Ingredients for Sustainable Cosmetics. *Cosmetics*, 7(2), 46, (2020).
- Akyol N.H., Yolcubal I., Oxidation of Nonaqueous Phase Trichloroethylene with Permanganate in Epikarst Water Air Soil Pollut. 224:1573, 1(2013).
- Akyol N.H., Turkkan S., Effect of cyclodextrin-enhanced dissolution on mass removal and mass discharge reduction for TCE source zones in heterogeneous porous media Water Air Soil Pollut. 229(2) 30. (2018).
- Akyol N.H., Surfactant-enhanced permanganate oxidation on mass-flux reduction and mass removal (MFR-MR) relationships for pool-dominated TCE source zones in heterogeneous porous media Water Air Soil Pollut. 229: 285 (2018)
- Akyol N.H., Lee A.R., Brusseau M.L., Impact of enhanced-flushing reagents and organic liquid distribution on mass removal and mass discharge reduction Water Air Soil Pollut. 224(10), 1731. (2013).
- Albino J.D., Nambi I.M., Effect of biosurfactants on the aqueous solubility of PCE and TCE J Environ Sci Health A Tox Hazard Subst Environ Eng, 44:14, 1565(2009).
- Booth J.M., Tick G.R., Akyol N.H., Greenberga R.R., Zhang Y., Experimental comparison of agent-enhanced flushing for the recovery of crude oil from saturated porous media J. Contam. Hydrol. 223 103471 (2019).
- Boving T.B., Brusseau M.L., Solubilization and removal of residual trichloroethene from porous media: comparison of several solubilization agents J. Contam. Hydrol. 42, 51–67 (2000)
- Brusseau M.L., Matthieu D. E., Carroll K.C., Mainhagu J., Morrison C., McMillan A., Russo A., Plaschke M., Characterizing long-term contaminant mass discharge and the relationship between reductions in discharge and reductions in mass for DNAPL source areas J. Contam. Hydrol. 149, 1 (2013).
- Chen J., Wu Q., Hua Y., Chen J., Zhang H., Wang H., Potential applications of biosurfactant rhamnolipids in agriculture and biomedicine Appl Microbiol Biotechnol. 101(23), 8309 (2017).
- Dashtbozorg S.S., Invally K., Sancheti A., Ju K.L., Microbial biosurfactants and their environmental and industrial applications, 1<sup>st</sup>Edt. '018 (CRC Press) 56 (2019). ISBN 9781315271767
- DiFilippo E.L., Carroll K.C., Brusseau M.L., Impact of organic-liquid distribution and flow-field heterogeneity on reductions in mass flux J. Contam. Hydrol. 115, 14–25 (2010).
- Ghosh J., Tick G.R., Akyol N.H., Zhang Y., A pore-scale investigation of heavy crude oil trapping and removal during surfactant-enhanced remediation J. Contam. Hydrol. 223, 103471, (2019).

- 484 Harendra S., Vipulanandan C., Effects of Surfactants on Solubilization of Perchloroethylene  
485 (PCE) and Trichloroethylene (TCE) Ind. Eng. Chem. Res. 50, 5831–5837 (2011).
- 486 Helmy Q., Gustiani S., Mustikawati A.T., (2020, April). Application of  
487 rhamnolipid biosurfactant for bio-detergent formulation. In IOP Conference Series: Materials  
488 Science and Engineering (Vol. 823, No. 1, p. 012014) (2020).
- 489 Jadhav J.V., Anbu P., Yadav S., Pratap A.P., Kale S.B., Sunflower Acid Oil-Based Production  
490 of Rhamnolipid Using *Pseudomonas aeruginosa* and Its Application in Liquid Detergents J  
491 Surfactants Deterg., 22(3), 463(2019).
- 492 Kennedy C.A., Lennox W.C., A pore-scale investigation of mass transport from dissolving  
493 DNAPL droplets, J. Contam. Hydrol. 24, 221 (1997).
- 494 Kile D.E., Chiou C.T., Water solubility enhancements of DDT and trichlorobenzene by some  
495 surfactants below and above the critical micelle concentration Environ. Sci. Technol. 23, 7,  
496 832 (1989).
- 497 Mahal M.K., Murao A., Johnson G.R., Russo A.E., Brusseau M.L., Non-ideal Behavior  
498 During Complete Dissolution of Organic Immiscible Liquid: 2. Ideal Porous Media Water Air  
499 Soil Pollut., 213, 191 (2010).
- 500 Mata-Sandoval J.C., Karns J., Torrents A., Influence of rhamnolipids and triton X-100 on the  
501 biodegradation of three pesticides in aqueous phase and soil slurries. J Agric Food Chem  
502 49:3296, (2001)
- 503 Randhawa K.K.S., Rahman P.K.S.M., biosurfactants-past, present, and future scenario of  
504 global market. Front Microbiol 5, 454, (2014)
- 505 Rathankumar A.K., Saikia K., Ribeiro M.H., Cheng C.K., Purushothaman M.,  
506 kumar Vaidyanathan V., Application of statistical modeling for the production of highly pure  
507 rhamnolipids using magnetic biocatalysts: Evaluating its efficiency as a bioremediation  
508 agent J. Hazard. Mater. 412, 125323. (2021).
- 509 Russo A.E., Mahal M.K., Brusseau M.L., Nonideal behavior during complete dissolution of  
510 organic immiscible liquid: 1. Natural porous media J. Hazard. Mater. 172, 208 (2009).
- 511 Sajna K.V., Gottumukkala L.D., Biosurfactants in Bioremediation and Soil Health. In: Kumar  
512 A., Sharma S. (eds) Microbes and Enzymes in Soil Health and Bioremediation.  
513 Microorganisms for Sustainability, 16 vol (Springer, Singapore 2019).
- 514 Schwill F., Pankow J.F., Dense chlorinated solvents in porous and fractured media, (Lewis  
515 Publications, Chelsea, MI. 1988). pp. 144.
- 516 Strbak L. In Situ Flushing with surfactants and Cosolvents. US EPA, Washington,  
517 DC. <http://www.clu-in.org> (2000)
- 518 Tang S., Song X., Wang Q., Wang S., Review Adsorption behavior of organic pollutants on  
519 microplastics Chemosphere, 261, (2020)
- 520 Thakur P., Saini N.K., Thakur V.K., Gupta V.K., Saini R.V., Saini. A.K., Microb Cell Fact 20,  
521 1 (2021).



Tick G.R., Harvell J.R., Murgulet D, Intermediate-Scale Investigation of Enhanced-Solubilization Agents on the Dissolution and Removal of a Multicomponent Dense Nonaqueous Phase Liquid (DNAPL) Source Water Air Soil Pollut.226(11), (2015).

Zhong H., Zhang H., Liu Z., Yang X., Brusseau M.L, Zeng G., Sub-CMC solubilization of dodecane by rhamnolipid in saturated porous media Sci. Rep. 6, 33266 (2016).

Zhong L., Oostrom M., Contaminants in Vadose Zone Environments Vadose Zone Journal. 11,4 (2012).

Zhang Y., Miller R.M., Enhanced octadecane dispersion and biodegradation by a *Pseudomonas rhamnolipid* surfactant (biosurfactant).Appl. Environ. Microbiol. 58, 3276 (1992). PMC183091

Zhong H., Yang X., Tan F., Brusseau M.L, Yang L., Liu Z., Zeng G., Yuan X., Aggregate-based sub-CMC solubilization of *n*-alkanes by monorhamnolipid biosurfactant New J Chem.40(3), 2028 (2016)

Zhong H., Yang L., Zeng G., Brusseau M.L., Wang Y., Li Y., Liu Z., Yuan X., Tan F., Aggregate-based sub-CMC solubilization of hexadecane by surfactants RSC Adv. 5, 78142 (2015).

Yi G., Son J., Yoo J., Park C., Koo H., Rhamnolipid nanoparticles for in vivo drug delivery and photodynamic therapyNanomedicine NANOMED-NANOTECHNOL, 19, 12, (2019).

Xu Q., Nakajima M., Liu Z., Shiina T., Biosurfactants for microbubble preparation and applicationInt. J. Mol. Sci. 12, 1 462 (2011).

**Table 1.** Parameters for 2-D flow-cell experiments

Silica sand	v (cm/hr)	TCE injection	S <sub>n</sub> (%)	TCE Recovery (%)	Type of reagent
Experiment 1	6.54	Single Pool	0.002*	97.7	5% Rhamnolipid
Experiment 2	6.54	Double Pool	0.002*	98.3	5% Rhamnolipid
Experiment 3	6.54	Single Pool	0.001*	98.2	5% Rhamnolipid
Experiment 4	6.54	Single Pool	0.001*	97.6	2.5% Rhamnolipid
Experiment 5	6.54	Single Pool	0.002*	67.4	Water
Natural calcareous soil	v	TCE injection	S <sub>n</sub>	TCE Recovery	Type of reagent

	(cm/hr)		(%)	(%)	
Experiment 1	6.15	Single Pool	0.002*	98,4	5% Rhamnolipid
Experiment 2	6.15	Double Pool	0.002*	99.1	5% Rhamnolipid
Experiment 3	6.15	Single Pool	0.001*	97.2	5% Rhamnolipid
Experiment 4	6.15	Single Pool	0.001	98.1	2.5% Rhamnolipid
Experiment 5	6.15	Single Pool	0.002*	54.9	Water

\* $S_n$  is calculated as volume of TCE divided by pore volume of system

**Figure 1.** Image of organic-liquid distribution in tank system. A) First configuration with silica sand, B) Second configuration with natural calcarous soil

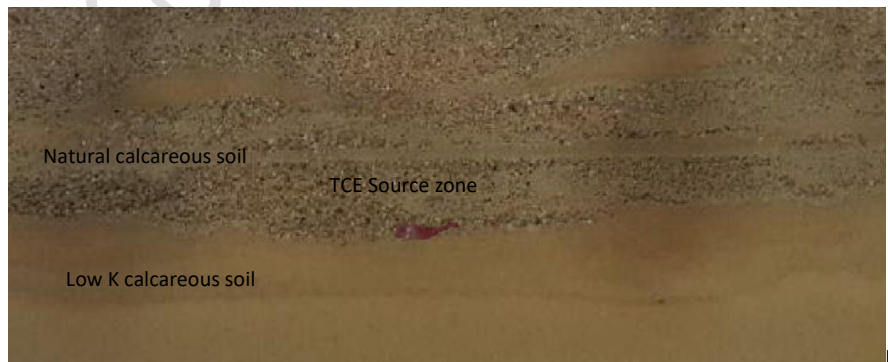
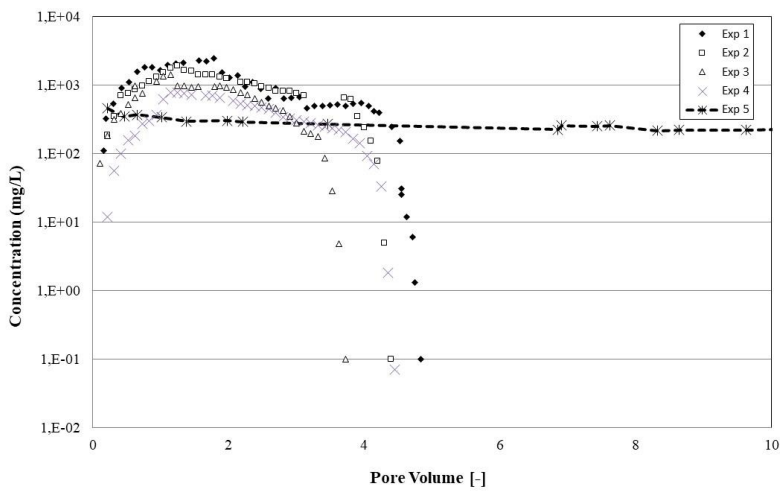
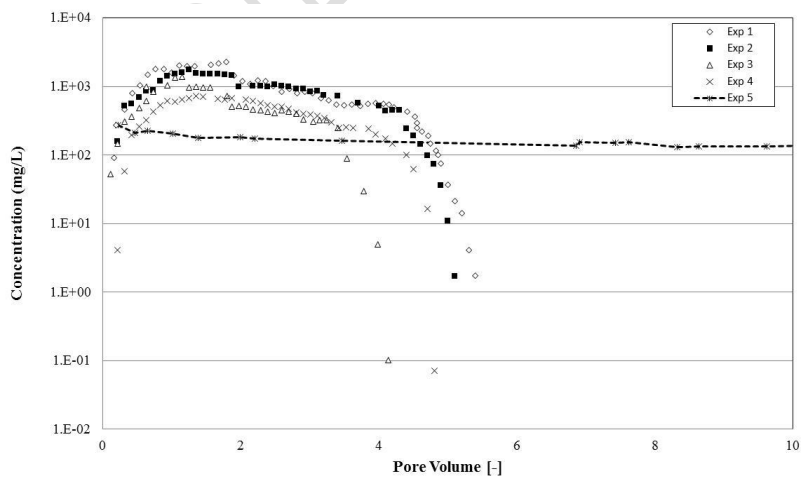


**Figure 2.** Effluent concentration as a function of the number of pore volumes for the dissolution and rhamnolipid enhanced-solubilization experiments using silica sand (1 PV= 3.67 hours) (Experiment 1, 2, 3, 4 and 5)



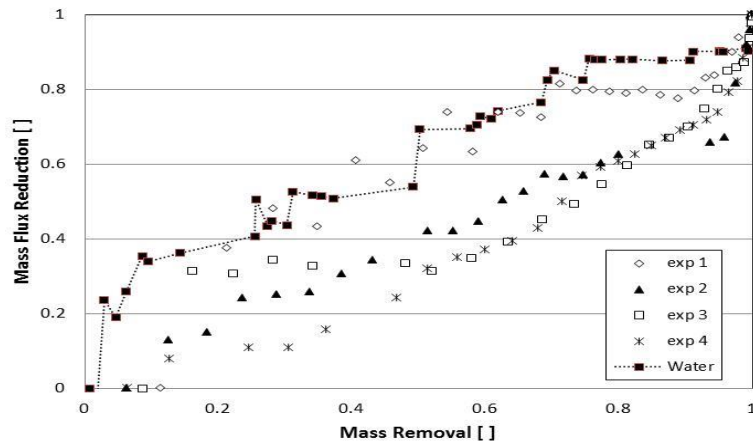
**Commented [A1]:** I think "[ ]" should be "[ - ]" for the X-axis title of Figure 2.

**Figure 3.** Effluent concentration as a function of the number of pore volumes for the dissolution and rhamnolipid enhanced-solubilization experiments using natural calcareous soil (1 PV= 3.90 hours) (Experiment 1, 2, 3, 4 and 5)



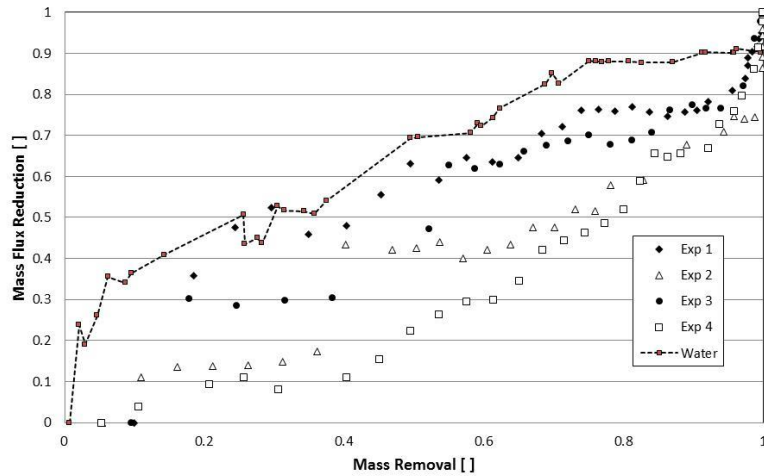
**Commented [A2]:** I think "[ ]" should be "[ - ]" for the X-axis title of Figure 3.

**Figure 4.** Mass-flux reduction versus mass removal relationships for rhamnolipid and water flushing tank experiments (First configuration)



**Commented [A3]:** I think "[ ]" should be "[ - ]" for the X-axis title and the y-axis title of Figure 4.

**Figure 5.** Mass-flux reduction versus mass removal relationships for rhamnolipid and water flushing tank experiments (Second configuration)



**Commented [A4]:** I think "[ ]" should be "[ - ]" for the X-axis title and y-axis title of Figure 5.